

See discussions, stats, and author profiles for this publication at: <https://www.researchgate.net/publication/257125178>

Ab initio study on the excited state proton transfer mediated photophysics of 3-hydroxy-picolinic acid

ARTICLE *in* CHEMICAL PHYSICS · DECEMBER 2012

Impact Factor: 1.65 · DOI: 10.1016/j.chemphys.2012.10.001

CITATIONS

5

READS

14

2 AUTHORS:



[Michal F Rode](#)

Institute of Physics of the Polish Academy o...

31 PUBLICATIONS 420 CITATIONS

SEE PROFILE

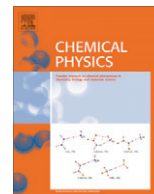


[Andrzej L. Sobolewski](#)

Polish Academy of Sciences

179 PUBLICATIONS 6,509 CITATIONS

SEE PROFILE



Ab initio study on the excited state proton transfer mediated photophysics of 3-hydroxy-picolinic acid

Michał F. Rode*, Andrzej L. Sobolewski

Institute of Physics, Polish Academy of Sciences, Al. Lotników 32/46, 02-667 Warsaw, Poland

ARTICLE INFO

Article history:

Received 5 July 2012

In final form 7 October 2012

Available online 24 October 2012

Keywords:

3-Hydroxy-picolinic acid

Excited-state proton transfer

Molecular photophysics

Ab initio calculations

ABSTRACT

The photophysics of 3-hydroxy-picolinic acid (3-hydroxypyridine-2-carboxylic acid) has been investigated with the aid of theoretical quantum chemistry methods. It is shown that the carboxylic group of the system serves as a transmitter of the proton between the oxygen atom of the hydroxyl group and the nitrogen atom of the ring. The two-dimensional minimum-energy potential-energy surfaces computed for the ground state and for the two lowest $^1\pi\pi^*$ and $^1n\pi^*$ excited states stress the importance of conical intersections between the states in governing the photophysics of this system.

© 2012 Elsevier B.V. All rights reserved.

1. Introduction

3-Hydroxy picolinic acid (3HPA) is widely used as a UV-sensitive matrix for oligonucleotides and other fragile biological systems in MALDI (matrix-assisted laser desorption) mass spectrometry analysis [1,2]. The 3HPA-based matrix shows significant improvement over many other MALDI matrices in terms of mass range available, signal-to-noise ratio, and the ability to analyze mixed base oligomers [3]. Despite of its practical utility not much is known about the photophysics of this molecule. Experimental spectroscopic data for this system are not available to our best knowledge hence, theoretical exploration of its photophysical-relevant reaction pathways may be of significant interest.

Since 3HPA possesses two proton donating moieties (hydroxyl groups) and two proton accepting (oxo- and azine-) spots, the most stable isomers of this compound contain two intramolecular hydrogen bonds. Apart from the 'open' isomers (with one or both hydrogen bonds broken) the four possible 'closed' (hydrogen-bonded) structures of 3HPA, schematically shown in Scheme 1, are related to each other by transfer of a single or both 'mobile' protons along the hydrogen bridges. The four isomeric structures of 3HPA considered in this work (Scheme 1) represent two photo-tautomeric pairs: Enol/Oxo – with respect to protonation of the O_1 atom, and Imino/Amino – with respect to protonation of the N_1 atom. First initials of these tautomeric names are used hereafter for the short-hand labeling of a given tautomer.

In the view of the above statements, it is thus very likely that photophysics of the isolated 3HPA (in the gas phase or in the inert-gas matrix environment) is dominated by the Excited-State Intramolecular Proton Transfer (ESIPT) process. The ESIPT reaction is of particular interest since it is very fast photophysical process and often ensures the nonradiative deactivation mechanism via a conical intersection (CI) between the excited (S_1) and the ground (S_0) electronic states. These properties appear to play an essential role in so-called organic photostabilizers [4] which are in widespread technical use for the protection of plastics and other light-sensitive materials against degradation by the UV components of sunlight [5,6]. The most commonly used as organic photostabilizers are derivatives of 2-hydroxybenzophenone and 2-(2'-hydroxyphenyl)benzotriazole. These compounds exhibit high absorption coefficients in the near-UV region and have a nondegradative pathway for rapid return to the ground electronic state. In one of the best commercial photostabilizers (TINUVIN-P) the photophysical cycle is completed on a subpicosecond timescale [7].

It is thus very likely that the ESIPT process provides the base for the application of 3HPA as the UV-sensitive matrix for the laser desorption spectroscopy. Due to this process, absorbed UV light is very fast turned into the heat of vibrations in the molecular ground state (perhaps on the subpicosecond time scale) which evaporates the matrix and the deposited biomolecules. The molecular photostability of 3HPA-matrix associated with this process secures the fragile biomolecules against the undesired photochemical reactions with fragmented radicals of 3HPA molecules.

The nonradiative decay mechanism in ESIPT systems is usually related to the twisting motion of the two molecular moieties, namely: the proton-donating and proton-accepting units [8,9].

* Corresponding author.

E-mail address: mrode@ifpan.edu.pl (M.F. Rode).

Femtosecond experiments performed for one of such compounds (7-(2-pyridyl)indole) confirm these theoretical predictions [10]. The intramolecular twisting stabilizes the excited state of the proton-transferred form and, at the same time, destabilizes the ground electronic state along this reaction coordinate. In effect this promotes the non-adiabatic transition between the S_1 and S_0 states due to small or vanishing energy gap near the perpendicular orientation of the two molecular moieties with respect to each other. This results in the fast return to the nominal-starting form after the whole photocycle process completes, if the system possesses one distinguishable minimum on the ground-state potential energy surface.

However, when the ESIPT molecule exhibits bifunctional photochromic property i.e. it has two (or more) stable tautomeric minima in the S_0 then such system might be considered as promising candidate for optical-switching or data-storage device (for reviews see Refs. [11,12] and references therein).

Recently, one of us (ALS) has proposed a new class of the ESIPT-based organic functional molecules [13]. The mechanistic principle of the functionality of these systems involves the optically induced transfer of a proton between two remote covalently-bound spots of an aromatic molecule, the so-called molecular ‘frame’, with the aid of a mobile molecular moiety called as the proton ‘crane’. The molecular crane picks up the proton from the acidic moiety of the molecular frame due to optical excitation and by the twisting delivers it to the basic moiety of the frame dropping the proton at the conical intersection with the ground state near the perpendicular conformation of the crane with respect to the planar aromatic frame.

The prototype of the optically driven molecular switch based on the ESIPT phenomenon was theoretically characterized in Ref. [13] on the example of the 7-hydroxy-(8-oxazine-2-one)-quinoline, in which the oxazine moiety acted as a proton crane, linked to the 7-hydroxy-quinoline as a molecular frame. The photo-physics of the first functional system synthesized according to theoretical prescription, 7-hydroxy-8-carbaldehyde-4-methyl-quinoline, was investigated in the Ar-matrix isolation UV/IR spectroscopy [14].

Unlike in the twist-based ESIPT processes discussed above, the ESIPT process involved in the photophysics of the 3HPA molecule is expected to be of different mechanistic nature. In this system the ‘proton-crane’ unit, such as carbaldehyde [14] or pyridine [15] moiety as discussed above, is replaced by the ‘proton-transmitter’ unit; the carboxylic group. Thus the transfer of a proton between the two remote spots of the pyridine ring (structures **EI** and **OA** of Scheme 1) do not need any large amplitude motion of the transmitting carboxyl group, but may only involve a sequential or concerted transfer of two protons.

The idea of double-ESIPT (DESIPT) process refers to early works on [2,2′-bipyridyl]-3,3′-diol (BP(OH)₂) and its derivatives and more recently to photophysics of indigo, where it was unequivocally shown that such process takes place [16–19]. These systems were also studied theoretically mainly with respect to the question of the sequential vs. concerted DESIPT [20–22]. More recently occurrence of the DESIPT process was proven for the 7-hydroxy-quinoline-8-carboxylic acid (7HQCA) [23]. In the latter system the 8-carboxylic group plays the role of a proton transmitter between the 7-hydroxyl group and the nitrogen atom of quinoline. This is very similar situation as in the 3HPA molecular system. The smaller size of 3HPA as compared to 7HQCA allows us to study in more detail the potential-energy landscape of the ground state and of the lowest excited states with respect to the DESIPT process and to provide a deeper insight into the basic principles which determine the photophysics of such systems.

2. Computational details

Equilibrium geometries of the molecular systems in their closed-shell singlet ground electronic state (S_0) were determined with the MP2 method [24]. Excitation energies, equilibrium geometries, and response properties of the lowest excited singlet states were calculated using the CC2 method [25,26] making use of the analytic gradients implemented for excited state optimization [27].

Correlation-consistent Valence Double Zeta basis set with polarization functions on all atoms (cc-pVDZ) [28] was used in calculations when not specified otherwise. Additionally, geometry optimizations were performed with the cc-pVDZ basis set augmented with diffuse functions (aug-cc-pVDZ) [28] in order to better reproduce the geometries of the intramolecular bonds in the molecule and the relative energies of the stable forms as well as the barrier between these forms in the S_0 state. To check the performance of the assumed methodology also Polarized Valence Triple Zeta basis set (cc-pVTZ) [28] was used in calculations of adiabatic S_1 energies and vertical excitation energies of the system. The basis set effect is discussed in more detail in the Electronic Supporting Information (ESI).

The minimum potential-energy surfaces along the distinct intramolecular coordinates relevant for transfer of the ‘mobile’ protons of the system were determined with the aid of the MP2 method for the ground state, and with the CC2 method for the excited states. The two intramolecular distances, O₁H and N₁H, were chosen as the proton transfer coordinates (see Scheme 1 for enumeration of atoms). For fixed values of these two distances, all other nuclear degrees of freedom were optimized under constraints of the C_s symmetry.

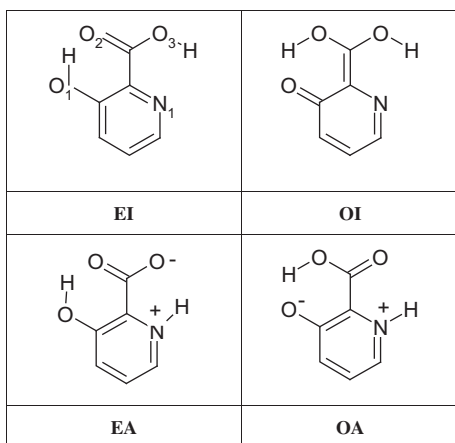
All calculations were performed with the TURBOMOLE program package [29], making use of the Resolution-of-the-Identity (RI) approximation for the evaluation of the electron-repulsion integrals [30]. Exceptions were the structures corresponding to the transition states between relevant S_0 -minima and the conical intersections between the states which were optimized with the MP2 and CASSCF methods, respectively, with the aid of the Gaussian g09 program package [31].

3. Results and discussion

3.1. Ground-state stable structures of 3HPA and absorption spectra

The 3HPA molecular system, has two different minima in the ground electronic state S_0 : the **EI**(S_0) and the **OA**(S_0) forms presented in Scheme 1. The two intramolecular hydrogen bonds: O₁–H–O₂ and O₃–H–N₁ enforce their planar geometries. These two forms differ from each other by the position of the mobile protons attached either to the oxygen atom of the 3-hydroxy group or to the nitrogen atom of the pyridine ring, and thus represent the hydroxy- and oxo- (or enol and keto) tautomeric forms of the system. The other conformers of the system with broken hydrogen bonds are at least 0.8 eV higher in energy and are not relevant for the photophysical behavior investigated in this work.

The vertical excitation energies (ΔE^{VE}) of the first five lowest electronically excited states for both tautomeric forms calculated with the cc-pVDZ basis set are collected in Table 1, while the respective ΔE^{VE} values calculated with the aug-cc-pVDZ basis set are gathered in Table S1 of the ESI. The lowest vertical excitation energy ΔE^{VE} for the dipole allowed $S_0 \rightarrow {}^1\pi\pi^*$ transition for the **OA** form of 3.54 eV ($\lambda_2 = 350$ nm) (CC2/cc-pVDZ) is noticeably red-shifted with respect to 4.48 eV ($\lambda_1 = 277$ nm) value computed for the ‘nominal’ **EI** tautomer. This difference of about 1 eV in the excitation energy between the two tautomeric forms indicates on



Scheme 1. Tautomeric structures of 3HPA considered in this work with enumeration of atoms indicated.

the expected photochromism of the system. What distinguishes the keto form from the enol one is the fact that the ${}^1n\pi^*$ state for the former lies below the $2A'(\pi\pi^*)$ state. This is quite common situation for the enol/keto tautomeric systems of this size, and as it will be shown later, this low-lying ${}^1n\pi^*$ state is important for photophysics of photo-isomerization process.

3.2. The energetical landscape of the ground electronic state

The **EI** tautomeric form represents a global minimum on the ground-state potential-energy surface (PES) of the 3HPA system; Its tautomeric partner, **OA**(S_0), which is related to **EI** by transfer of two protons along the carboxylic bridge, is less stable by 0.44 eV at the MP2/cc-pVDZ level of theory (c.f. Fig. 1 and Table 2). To estimate the barrier separating these two forms, the transition-state structure **TS**(S_0) was optimized and was confirmed as the first-order saddle point between the **EI**(S_0) and **OA**(S_0) minima by computing the Hessian. The barrier for the tautomeric reaction in the S_0 state leading from the **EI**(S_0) to the **OA**(S_0) form was estimated to be of 0.78 eV, while the barrier for the back-reaction is of 0.34 eV.

The **TS**(S_0) structure, which resembles the **EA** form of Scheme 1 (its Cartesian geometry is given in ESI), is of a zwitterionic nature having deprotonated carboxylic group with both protons attached to the oxygen and nitrogen atoms of the pyridine ring, respectively. Interestingly, the structure with protonated carboxylic group (**OI**), which could also be expected as the another transient structure between the **EI**(S_0) and **OA**(S_0) minima, does not exist as the first-order saddle point (SP) on the PES of the ground state.

Table 1

Vertical excitation energy (ΔE^{VE} , in eV), oscillator strength (f), and dipole moment (μ , in Debye) of the lowest excited singlet states of the **EI** and **OA** forms of 3HPA, determined with the CC2/cc-pVDZ method at the respective ground-state equilibrium geometry.

EI (S_0)				OA (S_0)			
State	ΔE^{VEa}	f	μ	State	ΔE^{VEb}	f	μ
S_0	–	–	3.8	S_0	–	–	6.1
$S_1(\pi\pi^*)$	4.48	0.113	3.5	$S_1(n\pi^*)$	3.37	$<10^{-4}$	3.3
$S_2(n\pi^*)$	4.79	0.001	0.7	$S_2(\pi\pi^*)$	3.54	0.128	4.7
$S_3(n\pi^*)$	5.61	0.001	2.8	$S_3(n\pi^*)$	4.55	$<10^{-4}$	5.1
$S_4(\pi\pi^*)$	5.95	0.067	3.5	$S_4(\pi\pi^*)$	5.11	0.091	4.8
$S_5(\pi\pi^*)$	6.73	0.308	5.8	$S_5(\pi\pi^*)$	5.92	0.004	4.2

^a Relative to the energy of the S_0 -global minimum, **EI**(S_0) form.

^b Relative to the energy of the **OA**(S_0) equilibrium geometry.

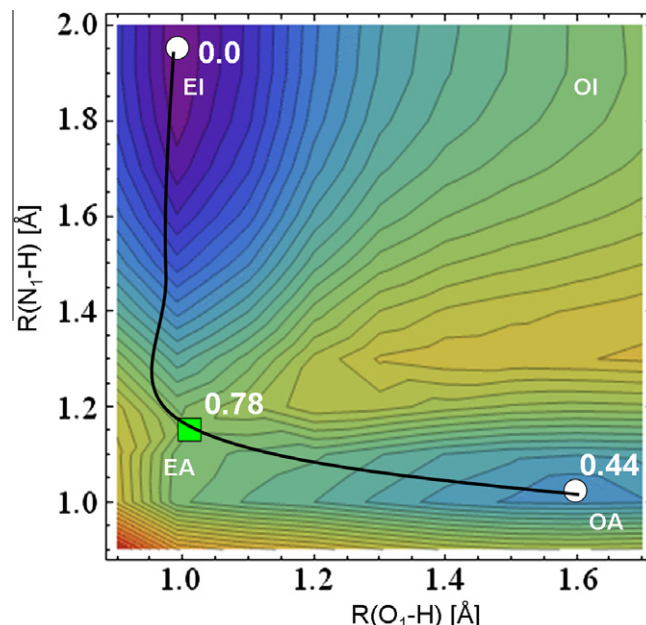


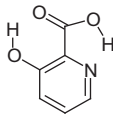
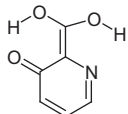
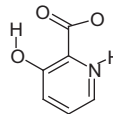
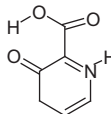
Fig. 1. Minimum-potential-energy surface of the ground electronic state of 3HPA plotted as a function of $R(O_1H)$ and $R(N_1H)$ coordinates. The isoenergy lines are plotted in the range 0.0–1.0 eV with the 0.05 eV step. The white circles on the surface represent the global, **EI**(S_0), and the local **OA**(S_0) minima, while the green square marks the **TS**(S_0) structure. The bold black line denotes the minimum energy path connecting the two tautomeric structures. The numbers denote energy of a given structure in eV. The results were obtained with the aid of the MP2/cc-pVDZ method. (For interpretation of the references to colour in this figure legend, the reader is referred to the web version of this article.)

In order to check this point in more detail, the minimum PES of the ground-state (MPES- S_0) was constructed as a function of the two intramolecular reaction coordinates: the O_1-H and N_1-H distances (see Scheme 1 for enumeration of atoms). The resulting two-dimensional surface is shown in Fig. 1. The positions of the two stable tautomeric forms (**EI** and **OA**) are indicated there by the white circles in the upper-left and the lower-right corners of MPES- S_0 , and the position of the **TS**(S_0) structure is indicated by the green square in the lower-left corner, respectively. Inspection of the shape of the surface shows a substantial barrier between the tautomeric minima along the diagonal of the Figure. The shape of MPES- S_0 precludes the existence of the **OI** form (abbreviated in the upper-right corner of Fig. 1) as the first-order saddle-point on the PES of the ground state. Thus the double-PT reaction connecting the **EI** and **OI** forms of 3HPA on the ground-state PES should be classified as the concerted asynchronous transfer of two protons via transient **EA** form due to stretching of the N_1-H and O_1-H bonds. The reaction is illustrated by the black line in Fig. 1. The lack of the potential-energy ‘valley’ near to the diagonal connecting the **EI** and **OA** minima in Fig. 1 (the saddle-point close to the center of the MPES- S_0) precludes the synchronous transfer of the protons [32].

3.3. The ${}^1\pi\pi^*$ and ${}^1n\pi^*$ excited-state minima

The lowest electronically excited singlet states of 3HPA are of the $\pi\pi^*$ and $n\pi^*$ orbital nature according to results shown in Table 1. These states fall into two categories distinguished by the symmetry of the orbitals; $\pi(A'')$ and $n(A')$ in the C_s symmetry point group. This symmetry holds strictly at the ground-state optimized minima, but the proximity of the ${}^1n\pi^*$ and ${}^1\pi\pi^*$ states may result in the symmetry breaking for the lower-lying excited state due to the coupling with the nearby lying state of different symmetry via the out-of-plane intramolecular vibrations. The vibronically

Table 2
Adiabatic energy (E_a , in eV), dipole moment (μ , in Debye) and oscillator strength (f) for transition to the ground state computed at the local minima on the PES of the lowest $^1\pi\pi^*$ and $^1n\pi^*$ excited states of 3HPA. Numbers in parentheses denote respectively fluorescence energy and dipole moment of the ground state computed at this geometry. The results were obtained with the MP2 (for S_0) and the CC2 (for excited states) methods with the cc-pVDZ basis sets. Adiabatic energy is defined relative to the global minimum, **EI**(S_0) form.

Tautomeric form				
	EI	OI	EA	OA
S_0				
E_a	0.0	–	0.78	0.44
μ	3.8	–	7.0	6.1
$^1\pi\pi^*$				
E_a	–	3.72 (2.55)	3.65 (1.92)	3.16 (1.91)
μ	–	1.6 (2.9)	2.2 (9.5)	3.9 (6.6)
f	–	0.095	0.024	0.034
$^1n\pi^*$				
E_a	4.21 (3.16)	3.51 (1.96)	2.64 (0.37)	2.77 (1.44)
μ	1.3 (4.8)	3.1 (2.8)	2.8 (10.0)	3.8 (6.3)
f	0.0002	$<10^{-4}$	$<10^{-4}$	$<10^{-4}$

induced interstate coupling may result in remarkable modification of the spectroscopic properties of the system. In the following, however, we are rather interested in a general photophysical behavior of the system than in description of its particular spectroscopic features. Thus henceforth the system is kept planar (C_s symmetry) if not specified otherwise. This allows us to characterize independently the PES of both lowest excited singlet states of the $\pi\pi^*$ and $n\pi^*$ orbital nature within the whole range of the intramolecular coordinates of the reactions studied.

Adiabatic energies of the stable (under the C_s symmetry constraints) local minima localized on the $^1\pi\pi^*$ and $^1n\pi^*$ PES are listed in Table 2. Inspection of the results shows that the energetical landscape of the lowest excited singlet states is much more complex than in the ground state. First of all, the four possible (hydrogen bonded) tautomeric forms of 3HPA listed in Scheme 1 represent local minima on the excited-state PES. The only exception is the **EI** tautomer in the $^1\pi\pi^*$ state which spontaneously relaxes to the **OI** form in the course of geometry optimization. Even though, the **EI**($n\pi^*$) minimum was localized in an unconstrained (but planar) geometry optimization, further study of the system revealed negligible barriers separating this from **EA**($n\pi^*$) and **OI**($n\pi^*$) minima. This result excludes the **EI**($n\pi^*$) minimum as having the physical meaning, since the zero-point energy (ZPE) correction is likely to be above the estimated barriers.

Additionally, in Table 2 the vertical energy gap to the ground state is listed at each of the optimized local minimum of the excited state. What is worth noticing when inspecting these data the **EA**($n\pi^*$) intermediate not only has the smallest adiabatic energy of 2.64 eV, but it also shows the smallest $^1n\pi^*$ - S_0 energy gap (of 0.37 eV) among all other optimized structures. This result may indicate on the presence of a conical intersection with the ground state in the vicinity of this structure, as it will be discussed later.

3.4. Photophysical scenarios

The major questions addressed in this paper are: (i) the possibility of population of the less stable **OA**(S_0) tautomer via the excited state reaction, and (ii) the elucidation of the mechanisms of the relevant photophysical processes.

As the eye-guide for discussion on photophysics of the 3HPA system, the data contained in Table 2 are additionally visualized in Figs. 2 and 3 in form of energy diagrams which illustrate two main scenarios expected to be relevant for photophysical behavior of the system upon UV excitation of the ground-state most stable

tautomeric form **EI**. Each of the two scenarios involve a sequential transfer of two protons via a single-PT excited-state intermediates; either through **OI** (Scenario 1, Fig. 2) or through **EA** (Scenario 2, Fig. 3). They differ from each other in the temporary sequence of the two PT events. While the Scenario 1 is initiated by the transfer of the proton from the 3-hydroxy group of the ring to the carboxy group of the carboxylic acid followed by the transfer of the another proton from the carboxy group to the azine nitrogen atom, the Scenario 2 is initiated by the latter process and followed by the former one. Both scenarios are topologically similar in a sense that; (i) the adiabatic energy of the $^1n\pi^*$ state (red solid lines) is below the adiabatic energy of the $^1\pi\pi^*$ state (blue solid lines) for the same molecular form of the system and (ii) the first step of the process, reaching the excited-state intermediate form (**OI** or **EA**, respectively), is exoergic from the side of the **EI** tautomer, both in the $^1n\pi^*$ and in the $^1\pi\pi^*$ excited states. However, with respect to the reverse process initiated by excitation of the **OA** tautomer, the reaction is down-hill only in the $^1n\pi^*$ state toward **EA**, but it is protected by a sizable barrier of 0.43 eV which makes this process rather unlikely to occur on the adiabatic PES of this state. Nevertheless, the vertical $\pi\pi^*$ -excitation of either **EI**(S_0) tautomer or the less stable **OA**(S_0) form provides enough access of energy (4.48 eV and 3.98 eV, respectively) to the system to dynamically overcome the barrier of adiabatic energy 3.20 eV (c.f. Fig. 3).

An important conclusion which emerges from inspection of Figs. 2 and 3 is that the **EA**($n\pi^*$) structure represents the global minimum on the excited-state PES. At the **EA**($n\pi^*$) excited-state minimum the 'vertical' energy of the ground state rises significantly and the $^1n\pi^*$ - S_0 energy gap is as small as 0.37 eV at the CC2/cc-pVDZ level of theory. This result provides strong evidence for the existence of a low-lying conical intersection between these states in the geometrical surrounding of this structure.

Indeed, the CASSCF optimization of the S_1 - S_0 conical intersection resulted in the structure shown in Fig. 4 (the Cartesian coordinates of this geometry are included in the ESI). As expected, this structure is related to the dioxo (**EA**) form, but also shows a significant out-of-plane displacement of the azine hydrogen atom. The sum of bond angles at the nitrogen atom is 339° and this clearly indicates on the change of hybridization at this atom from sp^2 to sp^3 . The active space for the CASSCF calculation comprised of six electrons in six orbitals (three HOMOs and three LUMOs HF-orbitals computed for the **EA**($n\pi^*$) C_1 -equilibrium geometry, *vide infra*).

The small or vanishing energy gap to the ground state indicates on the dominant role of internal conversion in (radiationless)

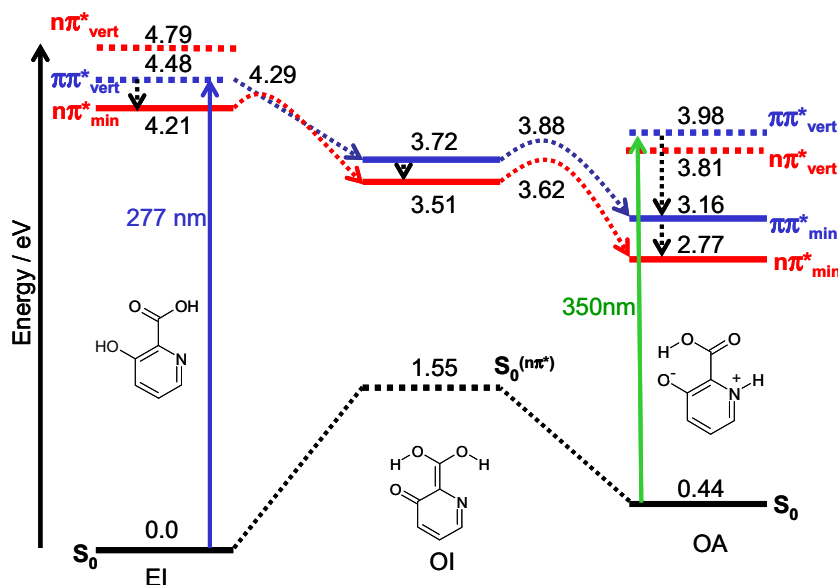


Fig. 2. Energy diagram illustrating photophysics of photo-tautomerization reactions in 3HPA driven by the PT processes according to Scenario 1. Electronic nature of the states is encoded by color: S_0 – black, the $^1\pi\pi^*$ – blue, and $^1n\pi^*$ – red. Solid lines represent adiabatic (optimized) energy of a given state while dashed blue and red lines represent ‘vertical’ excitation energy of a given state computed at the respective ground-state minimum. The dashed black line represents ‘vertical’ energy of the ground state computed at the optimized geometry of the **OI**($^1n\pi^*$) state. Vertical solid arrows indicate lowest dipole allowed absorption transitions. Dashed curved arrows denote relevant photophysical processes on a given PES, while vertical dashed arrows denote internal conversion. Numbers denote relevant energy in electron volts. The results were obtained with the aid of the MP2 and CC2 method for the ground and for the excited states, respectively. (For interpretation of the references to colour in this figure legend, the reader is referred to the web version of this article.)

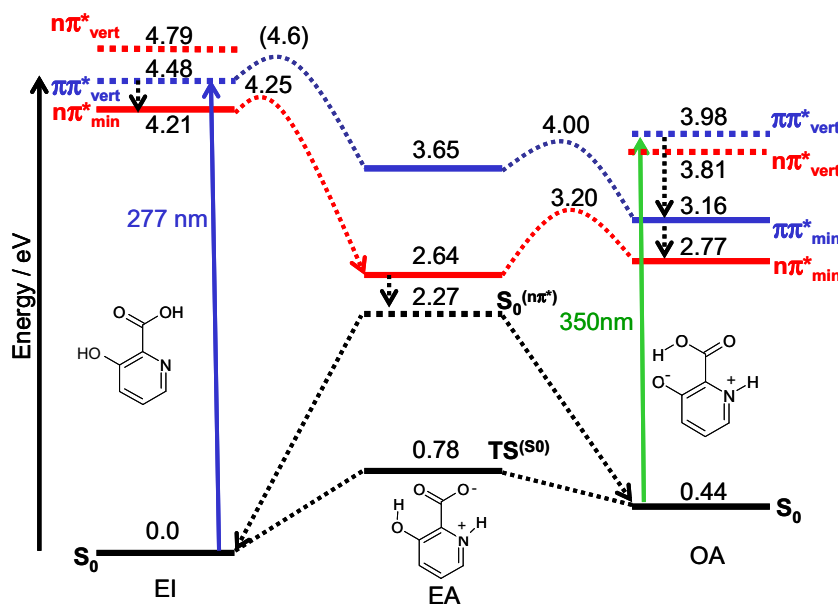


Fig. 3. The same as in Fig. 2, but illustrating Scenario 2.

depopulation of the excited states of the **EA** structure. This also concerns the second ‘transient’ structure (**OI**) for which, however, the $^1n\pi^*$ - S_0 energy gap is larger (~ 2 eV), but the $n\pi^*$ nature of the state and vanishingly small oscillator strength for the radiative transition to the ground state (see Table 2) precludes any measurable fluorescence to be observed from this form. Potentially emitting $\pi\pi^*$ -state of this form lies just above the **OI**($n\pi^*$) minimum and thus would undergo fast internal conversion to the latter state. This process is indicated in Fig. 2 by a vertical dashed arrow. One may notice upon inspection of Fig. 2 that the energy gap of ~ 2 eV may be a reason for much less effective internal conversion

from the **OI**($n\pi^*$) form to the ground state as compared to the **EA**($n\pi^*$) one. Instead, another, competitive and exoergic process may lead to the depopulation of the **OI**($n\pi^*$) form leading, through the **OA**($n\pi^*$) intermediate which is separated from the **OI**($n\pi^*$) by a barrier of only 0.11 eV (Fig. 2), to the population of **EA**($n\pi^*$) minimum (Fig. 3) which subjects to effective radiationless decay to the ground state, as discussed above. The only objection here is that even though, the **OA**($n\pi^*$) toward **EA**($n\pi^*$) reaction is exoergic, it needs activation energy of 0.43 eV (see Fig. 3). It is also worth to mention that the **EA**($n\pi^*$) form may easily be populated from the **EI**($n\pi^*$) minimum which is separated from the former one by a

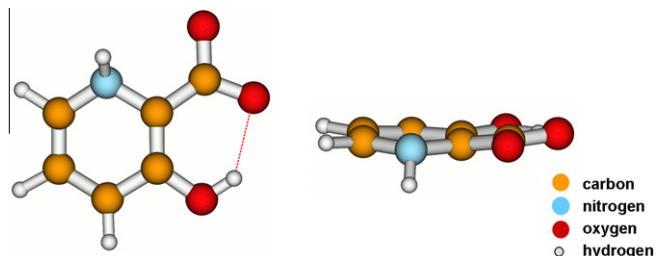


Fig. 4. Two views of the molecular structure of 3HPA optimized at the S_1 - S_0 conical intersection.

barrier of only 0.08 eV (see Fig. 3). To activate this reactive channel the **EI**($n\pi^*$) state must be populated. This may either happen due to intramolecular vibronic relaxation (IVR) of the initially excited $\pi\pi^*$ state leading to the population of the lower-lying $n\pi^*$ state in the **EI** form. Secondly, even if the system undergoes competing PT reaction along the barrierless path from the **EI**($\pi\pi^*$) toward the **OI**($\pi\pi^*$) minimum, the energy gap between the $\pi\pi^*$ and $n\pi^*$ states decreases since there is a barrier along the reaction path in the latter state, but not in the former one. Once the **EI**($n\pi^*$) state is populated the system may evolve either according to Scenario 1 or Scenario 2 as barriers on the $n\pi^*$ surface are in both directions negligibly small.

In summary, both ‘transient’ structures, **OI** and **EA**, which represent well defined minima on the PES of the lowest excited singlet state of 3HPA provide the source of very efficient radiationless deactivation of the system via Scenario 1 and 2, respectively. Since the internal conversion is expected to populate the ground state in vicinity of the **EA** structure, which represent transient state between the stable tautomeric forms **EI** and **OA** (Fig. 1), this provides a basic mechanism for photoinduced, and very likely reversible, transformation between these forms.

The C_s -optimized $^1A''(n\pi^*)$ minima are lower in energy than the corresponding $^1A'(\pi\pi^*)$ minima of the respective tautomeric forms of 3HPA, thus the vibronic coupling between these states caused by distortion of the system from the planarity induces a non-adiabatic relaxation of a wavepacket propagating on the optically ‘allowed’ $^1\pi\pi^*$ surface to the lower-lying ‘dark’ $^1n\pi^*$ surface. Such ordering of the lowest excited singlet states is also meaningful for the prediction that the system should not emit any measurable fluorescence at ambient conditions since according to Kasha’s rule optically excited system ends up in the lowest $^1n\pi^*$ excited state.

While in the case of the **EI** and **OI** S_1 minima, the equilibrium geometries obtained in the unconstrained optimization restore the C_s symmetry, the **OA**(S_1) minimum distorts the acidic group out of the plane with pyridine ring, and the **EA**(S_1) minimum shows a slight pyramidization at the N atom (the relevant excited-state-optimized geometries are listed in the ESI). The energetical effect of these geometric relaxations is less than a fraction of kcal/mol. These findings provide a clear motivation for investigation of the basic photophysical mechanism for the planar system. Additionally, this is also justified by the fact that the PT process is very fast and is generally much faster than any other nuclear motion, while both ground state equilibrium geometries are planar, thus any ESIPT process is initiated at the planar FC geometry. These results provide a strong motivation for further discussion of the photophysics within the C_s symmetry of the system.

In order to give more insight into the photophysical behavior of the system, 2-dimensional minimum-potential energy surfaces (MPES) of the lowest $^1\pi\pi^*$ and $^1n\pi^*$ singlet states spanned by the O_1 -H and N_1 -H distances and optimized at the CC2/cc-pVDZ level are shown in Figs. 5 and 6, respectively. The minima on the MPES are indicated by the red circles while the green squares denote transient structures. The numbers denote energy (in eV) of these

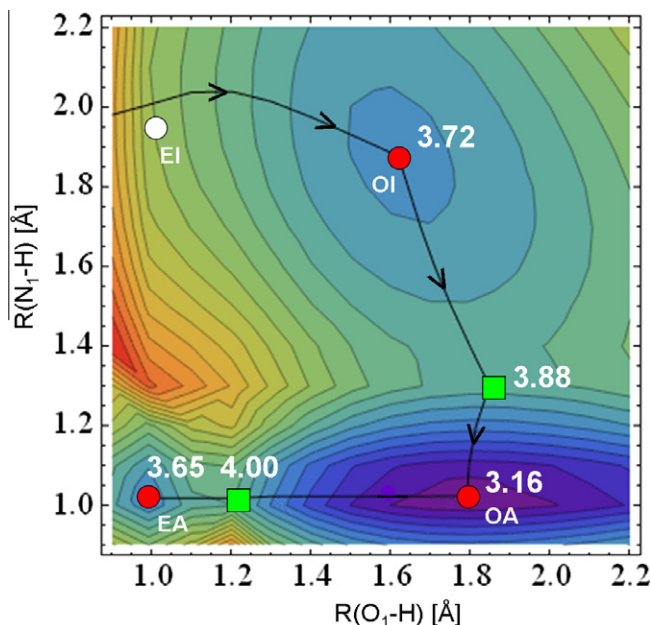


Fig. 5. Minimum-potential-energy surface of the $^1\pi\pi^*$ electronic state plotted as a function of $R(O_1H)$ and $R(N_1H)$ coordinates. The isoenergy lines are plotted in the range of 3.1–4.9 eV with the 0.1 eV step. The energy values at selected geometries are given in eV. The red circles represent the local minima, the green squares represent the transition-state structures, while the white circle represents the FC-region (the **EI**(S_0)-minimum). The bold black line represents the minimum energy path connecting the FC area with the minima through the transition-state structures. Arrows indicate the expected down-hill motion of the wavepacket. The results were obtained with the aid of the CC2/cc-pVDZ method. (For interpretation of the references to colour in this figure legend, the reader is referred to the web version of this article.)

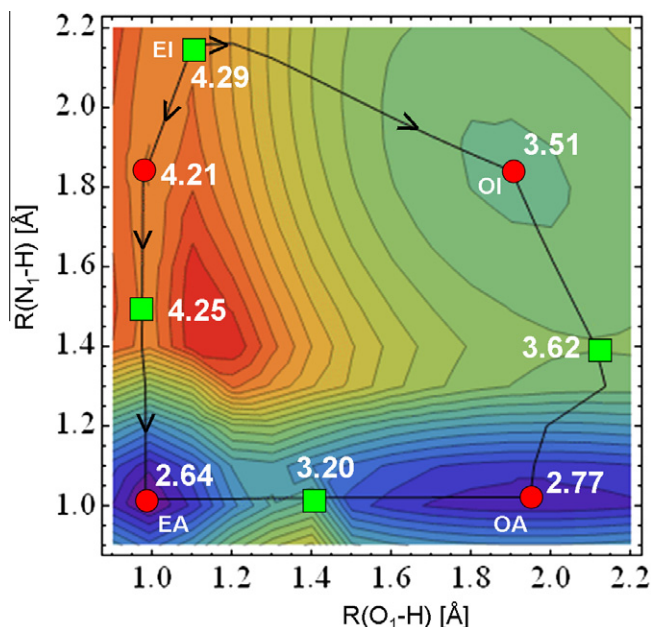


Fig. 6. Minimum-potential-energy surface of the $^1n\pi^*$ electronic state plotted as a function of $R(O_1H)$ and $R(N_1H)$ coordinates. The isoenergy lines are plotted in the range of 2.7–4.5 eV with the 0.1 eV step. The energy values of selected geometries are given in eV. The red circles on the surface represent the local minima and the green squares represent the transition-state structures. The bold black line represents the minimum energy path connecting the local minima through the transition-state structures. Arrows indicate the expected down-hill motion of the wavepacket. The results were obtained with the aid of the CC2/cc-pVDZ method. (For interpretation of the references to colour in this figure legend, the reader is referred to the web version of this article.)

points with respect to the global minimum of the ground state, $\text{EI}(S_0)$. The black line linking the minima (circles) through the barriers (squares) represent the minimum energy pathway illustrating the evolution of the system on a given MPES starting from the Franck–Condon (FC) region of the $\text{EI}(S_0)$ tautomer, indicated by the white dot in Fig. 5.

Let's first consider the Scenario 1 of the adiabatic process initiated by the UV excitation of the $\text{EI}(S_0)$ tautomer (ΔE^{VE} of 4.48 eV) to the $\pi\pi^*$ excited singlet state. The shape of the $^1\pi\pi^*$ MPES (Fig. 5) at the $\text{EI}(S_0)$ -FC-region (white circle) indicates on the barrierless ballistic motion of hydrogen atom toward the OI minimum (3.72 eV, see also Fig. 2). The evolution of this step of the ESIPT reaction is represented in Fig. 5 by the curved horizontal black line with arrows following the steepest descent path. By this barrierless reaction system reaches the local minimum OI , which is protected by only 0.16 eV (3.6 kcal/mol) from the global minimum of the $^1\pi\pi^*$ PES at the OA structure (3.16 eV). The small barrier and relatively large exoenergeticity of the reaction may result in a sequential transfer of the second proton as illustrated by the black vertical line with arrows in Fig. 5. However, what is more probable as discussed above, this process may already happen in the $n\pi^*$ state (see Fig. 2) and evolve the system to the $\text{OA}(n\pi^*)$ minimum of 2.77 eV.

The MPES of the $^1n\pi^*$ state, shown in Fig. 6, has similar landscape as that of the $^1\pi\pi^*$ state discussed above. The characteristic feature of the MPES of this state is presence of two almost isoenergetic minima, OA and EA , separated from each other by a sizable barrier of about 0.43 eV (see Figs. 3 and 6). Additionally, there is a broad plateau near the FC(EI) area with negligibly small barriers (1–2 kcal/mol) with respect to the neighboring EA and OI minima. Thus if the $^1n\pi^*$ state is populated near the FC area, this very likely will evolve adiabatically either in direction of the global minimum EA by a single PT (Scenario 2), or may reach the OA minimum by a sequential transfer of two protons (via the OI local minimum) (Scenario 1). In the former case a fast radiationless decay to the ground state is predicted since the S_1 – S_0 conical intersection is expected to lie in surrounding of the EA minimum of the $^1n\pi^*$ state as discussed above. If the system evolves via the second pathway reaching the OA global minimum via the OI local minimum, this may result in a very red emission (1.44 eV, 860 nm, Table 2). This is, however, rather unlikely because of negligibly small oscillator strength for this transition (Table 2), and the system is expected to decay to the ground state through intersystem crossing via triplet manifold.

The photophysical evolution of the system on the adiabatic PES of the $^1\pi\pi^*$ and $^1n\pi^*$ excited states has only approximate meaning because of a close proximity of these states. As this can already be noticed from inspection of the correlation diagrams shown in Figs. 2 and 3, intersections between the PES of these states are expected along the PT reaction coordinates. Strong non-adiabatic effects present at such intersections, or at the seams of intersections, will effectively dump the propagating wavepacket to the energetically lower PES.

In order to illustrate this effect, in Fig. 7, the $\min[\text{MPES}(^1\pi\pi^*), \text{MPES}(^1n\pi^*)]$ surface is plotted. Inspecting this figure one can notice that only in a limited area, near to the FC domain, the wavepacket is expected to evolve on the optically populated $^1\pi\pi^*$ PES and to be effectively dumped to the lower-lying $^1n\pi^*$ PES, precluding measurable fluorescence. One has to remember, however, that the “intersection seam” between the surfaces shown in Fig. 7 represents the so-called “apparent intersection” since both surfaces were independently optimized in intramolecular coordinates other than the PT coordinates spanning the surfaces. In any case, the “true” intersection seam between the surfaces is expected to lie in a close surrounding of this line.

The following “global” photophysical scenario of 3HPA can be constructed on the base of the computational results condensed in

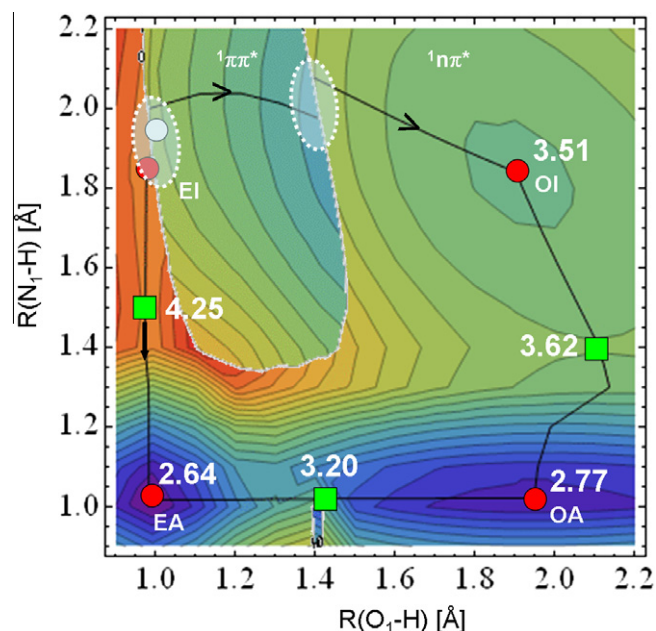


Fig. 7. The lower minimum-potential-energy surface of two excited electronic states: $^1\pi\pi^*$ (from Fig. 5) and $^1n\pi^*$ (from Fig. 6), $\min[{}^1\pi\pi^*, {}^1n\pi^*]$, plotted as a function of $R(\text{O}_1\text{H})$ and $R(\text{N}_1\text{H})$ coordinates. The red circles represent the local minima of the $^1n\pi^*$ MPES, while the white circle represents the $\text{EI}(S_0)$ -FC geometry. The bold black line illustrates the expected motion of the wavepacket from the FC area toward the local minima. The dashed white line denotes area, where degeneracy between the $\text{MPES-}^1\pi\pi^*$ and $\text{MPES-}^1n\pi^*$ occurs. The white-shaded ellipses indicate the regions, where the $^1\pi\pi^*$ – $^1n\pi^*$ non-adiabatic transition is expected most likely to occur. (For interpretation of the references to colour in this figure legend, the reader is referred to the web version of this article.)

Fig. 7. First of all one has to notice that the system excited in the FC area of the $^1\pi\pi^*$ PES can bifurcate into two different pathways; First, the non-adiabatic transition to the $^1n\pi^*$ state can take place because these states are essentially degenerate in the FC area. In fact, optical excitation is expected to populate the state of the mixed $\pi\pi^*/n\pi^*$ electronic nature. Thus the evolution on the $^1\pi\pi^*$ PES, as discussed above, can directly come into the play. This particularly concerns the direct access to the S_1 – S_0 conical intersection along the PT reaction coordinate leading to the EA tautomeric structure and resulting in radiationless decay to the ground state. Otherwise, part of the wavepacket may start the propagation on the $^1\pi\pi^*$ PES. Since the gradient in this state leads from the FC area in direction of the PT coordinate to the OI tautomeric structure, the non-adiabatic switching to the lower $^1n\pi^*$ PES is expected to occur on the way, and further evolution occurs on the PES of this state. The wavepacket reaching the OI local minimum can easily overcome the barrier and populate the OA minimum, where either an effective intersystem crossing to the triplet manifold may take place or the system can overcome the barrier to the EA global minimum and relax to the ground state through the nearby S_1/S_0 conical intersection.

To complete the photophysical cycle of 3HPA, the evolution on the ground-state PES has to be considered. As it was discussed above, the 3HPA system excited within the lowest singlet manifold is expected to return to the ground state on the radiationless way. The most effective $S_1 \rightarrow S_0$ internal conversion occurs in the area, where the PESs of both states are close to each other (a small S_1 – S_0 energy gap) or intersect (a conical intersection). Such “hot” area on the PES surfaces has been localized near to the EA form, which represents the transient structure between the two stable forms of 3HPA on the ground-state PES. At this transient structure the wavepacket can bifurcate and evolve in direction of the local minima either EI or OA . In such a way the photochemical transformation of 3HPA can take place.

4. Conclusions

Photophysics of 3-hydroxy-picolinic acid was investigated by means of *ab initio* electronic structure theory. The results point to the conclusion that the photophysics of the system is determined by the double ESIPT process which occurs for planar molecule and links two stable tautomeric forms of the system. Two dimensional potential-energy surfaces determined for the ground state and for the lowest excited ${}^1n\pi^*$ and ${}^1\pi\pi^*$ states stress the importance of an interplay between the close-lying states in governing the photophysical behavior of the system. Since the ${}^1n\pi^*$ state is found to lie below the ${}^1\pi\pi^*$ excited state for almost the whole area of the potential energy surface studied, the electronically excited system is expected to decay non-radiatively through conical intersections of the ${}^1n\pi^*$ state with the ground state, precluding measurable fluorescence from any tautomeric form of the system. These photophysical features are essential for MALDI experiments, where the whole energy of optical excitation should be effectively converted to the heat for the evaporation of the matrix.

Observation that the internal conversion populates the ground state of the system in vicinity of the **EA** transient structure linking the stable local minima **EI** and **OA** opens an intriguing question regarding the optical switching between these tautomeric forms. However, the **EI** and **OA** local minima of 3HPA are separated from each other by relatively small barrier of about 0.3 eV (≈ 7 kcal/mol), so they can effectively be thermalized at ambient conditions. The selective and reversible switching seems to be only feasible in a low-temperature matrix and for a selective excitation (optical burning) of the doorway tautomeric form [14]. Our recent study of the substituent effect on functionality of a molecular photo-switches [33] shows that the potential-energy landscape of such molecular system can effectively be modulated by a proper chemical tuning. These issues will be studied in more detail in the forthcoming paper.

Acknowledgments

This work has been supported by the research project of the National Science Centre of Poland, Grant No. 2011/01/M/ST2/00561, and by the computational grant G29-11 from the Interdisciplinary Centre for Mathematical and Computational Modeling (ICM) in Warsaw.

Appendix A. Supplementary material

Supplementary data associated with this article can be found, in the online version, at <http://dx.doi.org/10.1016/j.chemphys.2012.10.001>.

References

- [1] M. Karas, D. Bachmann, F. Hillenkamp, *Anal. Chem.* 57 (1985) 2935.
- [2] R.C. Beavis, B.T. Chait, *Rapid Commun. Mass Spectrom.* 3 (1989) 436.
- [3] K.J. Wu, A. Steding, C.H. Becker, *Rapid Commun. Mass Spectrom.* 7 (1993) 142.
- [4] J.-E.A. Otterstedt, *J. Chem. Phys.* 58 (1973) 5716.
- [5] H.J. Heller, H.R. Blattmann, *Pure Appl. Chem.* 30 (1972) 145.
- [6] H.J. Heller, H.R. Blattmann, *Pure Appl. Chem.* 36 (1973) 141.
- [7] M. Wiechmann, H. Port, F. Laermer, W. Frey, T. Elsaesser, *Chem. Phys. Lett.* 165 (1990) 28.
- [8] A.L. Sobolewski, W. Domcke, C. Hättig, *J. Phys. Chem. A* 110 (2006) 6301.
- [9] A.L. Sobolewski, W. Domcke, *Phys. Chem. Chem. Phys.* 8 (2006) 3410.
- [10] G.W.-S.Y. Nosenko, M. Kunitski, I. Petkova, A. Singh, W. J. Buma, R. P. Thummel, B. Brutschy, J. Waluk, *Angew. Chem.* 120 (2008) 6126; G.W.-S.Y. Nosenko, M. Kunitski, I. Petkova, A. Singh, W. J. Buma, R. P. Thummel, B. Brutschy, J. Waluk, *Angew. Chem. Int. Ed.* 47 (2008) 6037.
- [11] F.M. Raymo, *Adv. Mater.* 14 (2002) 401.
- [12] A.C. Benniston, *Chem. Soc. Rev.* 33 (2004) 573.
- [13] A.L. Sobolewski, *Phys. Chem. Chem. Phys.* 10 (2008) 1243.
- [14] L. Lapinski, M.J. Nowak, J. Nowacki, M.F. Rode, A.L. Sobolewski, *ChemPhysChem* 10 (2009) 2290.
- [15] C. Benesch, M.F. Rode, M. Čížek, R. Härtle, O. Rubio-Pons, M. Thoss, A.L. Sobolewski, *J. Phys. Chem. C* 113 (2009) 10315.
- [16] H. Bulska, *Chem. Phys. Lett.* 98 (1983) 398.
- [17] P. Borowicz, A. Grabowska, R. Wortmann, W. Liptay, *J. Lumin.* 52 (1992) 265.
- [18] P. Borowicz, A. Grabowska, A. Leś, Ł. Kaczmarek, B. Zagrodzki, *Chem. Phys. Lett.* 291 (1998) 351.
- [19] S. Yamazaki, A.L. Sobolewski, W. Domcke, *Phys. Chem. Chem. Phys.* 13 (2011) 1618.
- [20] A.L. Sobolewski, L. Adamowicz, *Chem. Phys. Lett.* 252 (1996) 33.
- [21] J.M. Ortiz-Sánchez, R. Gelabert, M. Moreno, J.M. Lluch, *ChemPhysChem* 9 (2008) 2068.
- [22] J.M. Ortiz-Sánchez, R. Gelabert, M. Moreno, J.M. Lluch, J.M. Anglada, J.M. Bofill, *Chem. Eur. J.* 16 (2010) 6693.
- [23] K.C. Tang, C.L. Chen, H.H. Chuang, J.L. Chen, Y.J. Chen, Y.C. Lin, J.Y. Shen, W.P. Hu, P.T. Chou, *J. Phys. Chem. Lett.* 2 (2011) 3063.
- [24] C. Möller, M.S. Plesset, *Phys. Rev.* 46 (1934) 618.
- [25] O. Christiansen, H. Koch, P. Jorgensen, *Chem. Phys. Lett.* 243 (1995) 409.
- [26] C. Hättig, F. Weigend, *J. Chem. Phys.* 113 (2000) 5154.
- [27] A. Kohn, C. Hättig, *J. Chem. Phys.* 119 (2003) 5021.
- [28] T.H. Dunning, *J. Chem. Phys.* 90 (1989) 1007.
- [29] R. Ahlrichs, M. Bär, M. Häser, M.H. Horn, C. Kölmel, *Chem. Phys. Lett.* 162 (1989) 165.
- [30] F. Weigend, M. Häser, *Theor. Chem. Acc.* 97 (1997) 331.
- [31] M.J. Frisch, G.W. Trucks, H.B. Schlegel, G.E. Scuseria, M.A. Robb, J.R. Cheeseman, G. Scalmani, V. Barone, B. Mennucci, G.A. Petersson, H. Nakatsuji, M. Caricato, X. Li, H.P. Hratchian, A.F. Izmaylov, J. Bloino, G. Zheng, J.L. Sonnenberg, M. Hada, M. Ehara, K. Toyota, R. Fukuda, J. Hasegawa, M. Ishida, T. Nakajima, Y. Honda, O. Kitao, H. Nakai, T. Vreven, J.A. Montgomery, Jr., J.E. Peralta, F. Ogliaro, M. Bearpark, J.J. Heyd, E. Brothers, K.N. Kudin, V.N. Staroverov, T. Keith, R. Kobayashi, J. Normand, K. Raghavachari, A. Rendell, J.C. Burant, S.S. Iyengar, J. Tomasi, M. Cossi, N. Rega, J.M. Millam, M. Klene, J.E. Knox, J.B. Cross, V. Bakken, C. Adamo, J. Jaramillo, R. Gomperts, R.E. Stratmann, O. Yazyev, A.J. Austin, R. Cammi, C. Pomelli, J.W. Ochterski, R.L. Martin, K. Morokuma, V.G. Zakrzewski, G.A. Voth, P. Salvador, J.J. Dannenberg, S. Dapprich, A.D. Daniels, O. Farkas, J.B. Foresman, J.V. Ortiz, J. Cioslowski, D.J. Fox, *Gaussian 09, Revision B.01*, Gaussian, Inc., Wallingford, CT, 2010.
- [32] M.J.S. Dewar, *J. Am. Chem. Soc.* 106 (1984) 209.
- [33] M.F. Rode, A.L. Sobolewski, *J. Phys. Chem. A* 114 (2010) 11879.